# Leveraging Spatial Reuse in 802.11 Mesh Networks with Enhanced Physical Carrier Sensing

Jing Zhu, Xingang Guo, L. Lily Yang, and W. Steven Conner
{jing.a.zhu, xingang.guo, lily.l.yang, w.steven.conner}@intel.com
Communication Technology Lab
Intel Corporation
2111 NE $25^{th}$ Ave., JF3-206
Hillsboro, OR 97124, U.S.A.

***Abstract*— Spatial reuse in a wireless network can allow multiple communications to proceed simultaneously, hence proportionally improve the overall network throughput. To maximize spatial reuse, the MAC protocol must enable simultaneous transmitters to maintain the minimal separation distance to avoid interference. This paper demonstrates that physical carrier sensing enhanced with tunable sensing threshold is effective at avoiding interference in 802.11 mesh networks without requiring the use of virtual carrier sensing through RTS/CTS. We present analytical model that demonstrates how to derive the optimal sensing threshold given reception power, data rate and network topology. Simulation results are shown for large-scale 802.11b networks to demonstrate that physical carrier sensing with the optimally tuned threshold improves network throughput by maximizing the potential of spatial reuse. In the case of a regular chain topology of 90 nodes, with tuned physical carrier sensing, the end-to-end throughput approaches 90% of the theoretical upper-bound that assumes a perfect MAC protocol. Hence, without modifying the 802.11 MAC protocol, our enhanced physical carrier sensing mechanism effectively maximizes the potential of improving network throughput with spatial reuse.**

## I. Introduction

Over the past few years we have witnessed the rapid proliferation of wireless LANs in various network environments. The need for higher data rates and improved coverage has led to at least two potential solutions to large-scale WLANs – multi-cell networks where each cell is serviced by its own access point (AP), and mesh networks where nodes work in ad-hoc mode and use multi-hop routing to relay each other's traffic. In both cases, the overall network throughput is proportional to the number of simultaneous communications that can be supported in the network. Co-channel spatial reuse allows simultaneous communications to reuse the same channel in spatially separated locations without interfering with each other.

A multi-cell WLAN is similar to a traditional cellular network – spatial reuse is often achieved through careful site planning and engineered channel assignment for each cell. In an ad-hoc network, however, no access point or base station exists to form such an infrastructure. Hence, engineered channel assignment is not feasible. Furthermore, because of the random nature of ad-hoc networks, detecting and avoiding interference is more complicated than in an infrastructure network. In [4], spatial reuse was demonstrated to depend on various characteristics of the network, including the type of radio, network topology, channel quality requirements and signal propagation environment. For each network configuration, there exists a minimum separation distance such that when simultaneous transmitters are separated by that distance, the maximum number of simultaneous transmissions can be accommodated, allowing maximum network throughput to be achieved. However, achieving maximum spatial reuse would require an ideal MAC protocol that schedules communication to maintain the optimal transmitter separation distance while minimizing interference.

Stations in most of today's WLANs run the IEEE 802.11 MAC protocol [1]. A transmitter uses carrier sensing to determine if the air medium (or channel) is busy before transmitting to avoid interference. Two types of carrier sensing are defined in the 802.11 MAC: mandatory physical carrier sensing that monitors the RF energy level in the air and optional virtual carrier sensing that uses the Request-to-Send/Clear-to-Send (RTS/CTS) handshake to ensure that the air medium is reserved prior to transmitting data frame. Virtual carrier sensing was designed to avoid the well-known hidden terminal problem [8], where it is assumed that physical carrier sensing at a transmitter is not sufficient to avoid interference at a receiver. However, it has been shown that virtual carrier sensing through RTS/CTS has fundamental limitations in avoiding interference from hidden terminals in mesh networks [9].

In this paper we demonstrate that, when properly tuned, physical carrier sensing is effective at avoiding interference in a multi-hop wireless mesh network, even without the use of virtual carrier sensing. In physical carrier sensing, a station samples the energy level in the air and starts a packet transmission only if the reading is below a carrier sensing threshold, indicating that no transmissions are taking place that could result in interference. As RF signal propagates, the reception energy level decays as the distance from a transmitter increases. Hence the carrier sensing threshold effectively determines the minimum distance between si-

 0-7803-8533-0/04/$20.00 (c) 2004 IEEE

multaneous transmitters. As stated previously, the optimal distance depends on various network properties, thus the carrier sensing threshold should also be tuned to match network conditions. However, most of today's 802.11 MAC implementations use a static threshold, or do not allow the threshold to be independently tunable [13]. As a result, physical carrier sensing often leads transmitters to be either too conservative or too aggressive when using the wireless channel.

Therefore, we argue that future 802.11 devices should allow the tuning of carrier sensing threshold. We illustrate through theoretical analysis how to derive the appropriate carrier sensing threshold from relevant network characteristics. Furthermore, we show that using the optimal carrier sensing threshold completely eliminates the hidden terminal problem. We present OPNET simulation results for two regular network topologies (chain and grid) to show that by tuning the physical carrier sensing threshold, the overall network throughput can be improved significantly compared to that of the legacy 802.11 MAC. Furthermore, the increased throughput can approach approximately 90% of the theoretical upper-bound predicted by spatial reuse study. Hence, using a tunable threshold not only improves network performance, but also maximizes the potential for improving network throughput through spatial reuse.

It is worth pointing out that performance improvement to 802.11 networks involves enhancement to various aspects of the 802.11 MAC protocol, and it has been the subject of extensive researches [6] [7] [11]. We believe that for any given network environment, the solution to maximizing network performance must be a careful combination of approaches addressing multiple aspects of the network behavior. Recommending that perfect combination for general 802.11 networks is beyond the scope of this paper. In this paper, we focus on leveraging spatial reuse to enhance the network performance.

The rest of this paper is organized as follows: Section II presents a SNIR-based communication model that is used for interference analysis. Section III introduces our analytical model for interference mitigation and optimal physical carrier sensing. Section IV presents OPNET simulation results demonstrating measurable benefit from tuned physical carrier sensing. Section V discusses related work, and finally we conclude the paper in section VI.

## II. Managing Interference with Carrier Sensing

In this section, we discuss the properties of radio communication that determine the effectiveness of carrier sensing and point out several shortcomings of the carrier sensing techniques commonly employed in 802.11 MAC.

### A. Communication model

Pathloss models are commonly used to describe the radio propagation property in wireless networks [14]. A typical pathloss model expresses the average signal strength at the receiver as a function of the T-R (transmitter-receiver) separation distance, $d$, i.e.

$$P_{rx}(d) = \bar{P}_{rx}\left(\frac{\bar{d}}{d}\right)^{\gamma} \quad (1)$$

where $\gamma$ is the pathloss exponent that characterizes how quickly a signal fades in the particular network environment. $P_{rx}(d)$ denotes the signal strength at a receiver at distance $d$ away. Finally, $\bar{P}_{rx}$ is the reference receiving signal strength as measured at the reference distance $\bar{d}$ (usually 1 meter).

The aggregate energy detected by a receiver consists of signal (from intended transmitter), interference (from unwanted transmitter(s)) and noise. In a WLAN such as an 802.11 network, a receiver can receive a packet with high probability of success only if the receiving strength of the intended signal is greater than a threshold (denoted by $P_R$), and the Signal-Noise-Interference Ratio (SNIR) is above a threshold (denoted by $S_0$).

$$\begin{cases} P_{rx}(d) \geq P_R \\ \frac{P_{rx}(d)}{P_N + \sum_i P_{rx}(d_i)} \geq S_0 \end{cases} \quad (2)$$

where $P_N$ is the strength of the ambient noise, and $P_{rx}(d_i)$ denotes the signal strength from interference source $i$ at distance $d_i$. In most cases, the noise level is negligible compared to either the signal and interference. Hence in the rest of paper, instead of SNIR, we only consider the Signal-Interference Ratio (SIR). Moreover, in a multiple data rate network such as the 802.11 narrowband network, a higher data rate normally requires a higher $S_0$.

### B. Interference model

According to (2), a successful reception depends on the receiving power as well as the runtime SNIR. Hence there does not exist a static *transmission range* irrespective to the network environment and runtime traffic pattern. Nonetheless, when there is no interference, the noise will determine the maximum distance for reception. Let transmission range denote that distance. For each network, we can assume such transmission range exists. Similarly, in the rest of the paper, let us use simplistic terms such as interference range, carrier sensing range, etc. to facilitate analysis.

Fig.1 shows a segment in a typical multi-hop mesh network with a reference transmission from TX to RX and four other nodes (A, B, C, and E). The same transmission power is used by every node in the network. We define the following notations:

$D$: T-R separation distance,

$R$: Transmission range, given by

$$R = \bar{d}\left(\frac{\bar{P}_{rx}}{P_R}\right)^{\frac{1}{\gamma}} \quad (3)$$

$I$: Interference range – an energy level equivalent to a transmitter within that distance of the receiver

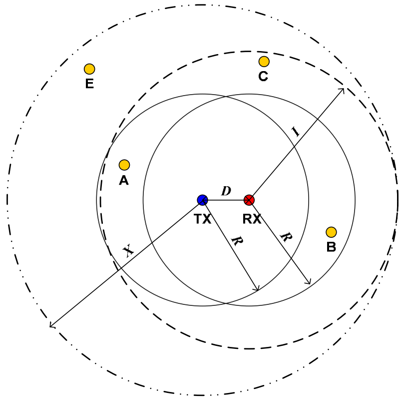


Fig. 1. Communication in a wireless mesh network

will disrupt the reception, given by

$$I = D\left[\frac{1}{S_0} - \left(\frac{D}{\bar{d}}\right)^{\gamma}\frac{P_N}{\bar{P}_{rx}}\right]^{-\frac{1}{\gamma}} \quad (4)$$

With negligible noise ($P_N = 0$), (4) becomes

$$I = S_0^{\frac{1}{\gamma}} D > D \quad (5)$$

$X$: Physical carrier sensing range – a transmitter will deem channel busy if it senses an energy level equivalent to a transmitter within that range, given by

$$X = \bar{d}\left(\frac{\bar{P}_{rx}}{P_C}\right)^{\frac{1}{\gamma}} \quad (6)$$

where $P_C$ denotes the carrier sensing threshold.

As seen from Fig.1, a transmission from either node A, B, or C would interfere the ongoing transmission between TX and RX.

### C. Limitation of Carrier Sensing in mesh network

In today's 802.11 networks, the physical carrier sensing (PCS) mechanism is typically configured with a fixed threshold, which is often very low such that even a remote communication would generate a signal strong enough to make a station withhold its transmission. As a result, very little spatial reuse is allowed. Moreover, the fixed threshold cannot be dynamically tuned according to different network conditions. As wireless networks being deployed at increasingly higher densities, the potential for spatial reuse increases. However, the current PCS scheme with fixed threshold limits the ability to make full use of spatial reuse in these dense wireless network scenarios.

The 802.11 MAC also defines a Virtual Carrier Sensing (VCS) mechanism [1] using the RTS/CTS handshake to avoid interference from hidden terminals. With VCS, TX sends out an RTS frame prior to the data transmission to reserve a channel usage time. RX responds with a CTS frame if it agrees with the request. In CTS RX also indicates the channel usage duration. Other nodes that overhear RTS or CTS will honor the reservation and not transmit. To receive RTS/CTS, a potential interfering node must be within the transmission range of TX (for RTS) or RX (for CTS). Unfortunately, (5) has indicated that there could be nodes outside of the transmission range that can still cause interference. Therefore, VCS is not always effective in a mesh network at suppressing interference from hidden terminals.

## III. Enhanced Physical Carrier Sensing

### A. Interference mitigation via Physical Carrier Sensing

With Physical Carrier Sensing (PCS), a station compares the energy level against the sensing threshold ($P_C$), and starts transmission only when the reading is below $P_C$. Hence $P_C$ determines how much interference a communication can tolerate and reflects a sensing range ($X$). In Fig.1, all potentially interfering nodes, including C, can be eliminated by enlarging the sensing range ($X$) to cover the entire interference area, i.e. $X \geq D + I$. Therefore, any node within the sensing range of TX will be able to detect the on-going transmission between TX and RX, therefore refrain from transmitting to avoid generating interference. Given (5) and (6), we have

$$\bar{d}\left(\frac{\bar{P}_{rx}}{P_C}\right)^{\frac{1}{\gamma}} \geq D\left(1 + S_0^{\frac{1}{\gamma}}\right) \quad (7)$$

The PCS threshold $P_C$ plays a key role in (7) to coordinate simultaneous transmissions for optimal spatial reuse. PCS generally is more robust than VCS since it does not require packets to be received correctly. It is also more flexible since the sensing range can be easily adjusted by tuning the PCS threshold. Nonetheless, it is worth pointing out that PCS still doesn't solve the *exposed terminal* problem. For example, even though a transmission by node E will not disrupt RX, because it is within the sensing range of TX, E will be able to *sense* the transmission and do not transmit. Having exposed terminal can potentially reduce the overall network throughput. However, by tuning the physical carrier sensing threshold, we can achieve the optimal tradeoff between hidden terminal and exposed terminals so as to obtain the best throughput.

### B. Optimal PCS threshold

In this paper, we study homogeneous networks with regular topology where neighboring nodes are separated by equal distance $D$. When communications are restricted to between neighboring nodes only, the receive strength of the intended signal, denoted by $P_D$, is also constant throughout the network. Let $p_{cs\_t} = \frac{P_C}{P_D}$, then (7) becomes

$$P_{cs\_t} \leq \beta, \quad \text{where} \quad \beta = \left(1 + S_0^{1/\gamma}\right)^{-\gamma} \quad (8)$$

To consider the optimal tradeoff with exposed terminal, let $\rho$ denote the ratio between the exposed terminal area and the whole PCS sensing area, then

$$\rho = \frac{\pi X^2 - \pi I^2}{\pi X^2} \approx \frac{D^2\left(1+S_0^{1/\gamma}\right)^2 - D^2 S_0^{2/\gamma}}{D^2\left(1+S_0^{1/\gamma}\right)^2} = 1 - \left(\frac{S_0^{1/\gamma}}{1+S_0^{1/\gamma}}\right)^2 \quad (9)$$

With $S_0^{1/\gamma} >> 1$ (more so for higher data rates since higher $S_0$ values will be required), we have $\rho \approx 0$ so that the exposed terminal problem can be ignored, and $\beta$ gives the optimal $p_{cs\_t}$. Let

$$\beta' = \frac{1}{S_0} \quad (10)$$

Notice that $\beta|_{S_0^{1/\gamma}>>0} \approx \beta'$. In fact, $\rho \approx 0$ means that the sensing area almost overlaps with the interference area, therefore the transmitter and receiver are essentially co-located. It's especially true for a pair of neighboring nodes in a large network. Hence they also observe near identical interference level, i.e.

$$P_S \approx P_I \quad (11)$$

where $P_S$ indicates the total power of signals sensed by the transmitter, and $P_I$ is the interference strength at the receiver.

In order to start a transmission, the total power sensed by a transmitter must be below the PCS threshold,

$$P_S \leq P_C \quad (12)$$

Also, the interference power at the receiver can not exceed the tolerable level for a successful transmission,

$$P_I \leq P_D/S_0 \quad (13)$$

Combining (11)∼(13) leads to

$$P_C \leq P_D/S_0 \quad (14)$$

Since a higher $P_C$ will result in more simultaneous transmissions, its upper bound in (14) will lead to the best spatial reuse. That corresponds to $p_{cs\_t} = 1/S_0$, i.e. $\beta'$. It's worth noting that $\beta'$ is independent of the path loss exponent $\gamma$. Hence the optimality of a sensing threshold is applicable regardless of the propagation environment where the network is set up.

### C. Optimal spatial reuse

The optimal spatial reuse is achieved when the maximum number of successful transmissions can be accommodated simultaneously. Spatial reuse will be determined by when, where and how much interference exists in the network at any given moment. Hence network topology, communication schedule and traffic load all affect the optimal spatial reuse.

In [4] the authors investigated spatial reuse from a physical layer perspective. They assumed a homogeneous environment where every transmitter uses the same transmission power and data rate, and communicates to an immediate neighbor at the constant T-R distance $d$. Under such conditions, spatial reuse can be characterized by the distance between neighboring simultaneous transmitters (T-T separation distance). The minimum T-T distance results in optimal spatial reuse. Optimal spatial reuse was investigated for two regular network topologies: the chain network and the grid network. Let $k$ denote the T-T distance, in number of hops (hop distance being $d$), then the lower bounds of $k$ for the two topologies are

$$\begin{cases} k \geq \left[2\left(1+\frac{1}{\gamma-1}\right)S_0\right]^{\frac{1}{\gamma}}, & \text{Chain network} \\ k \geq \left[6\left(1+\frac{1}{\gamma-2}\right)S_0\right]^{\frac{1}{\gamma}}, & \text{2-D grid} \end{cases} \quad (15)$$

### D. Aggregate throughput bound

If we assume a perfect MAC protocol that schedules simultaneous communications only on transmitters that are $k$ hops away from each other, the network will be able to accommodate the maximum number of simultaneous transmitters, hence reaching its aggregate throughput limit. From the lower bounds of $k$, we can extrapolate such aggregate throughput limits.

In a chain network of $N$ nodes, with each node communicating to its immediate neighbors, a packet from one end will be relayed by each of the $N-2$ intermediate nodes before reaching the other end. Since at most $N/k$ simultaneous transmitters can be supported in the chain. Let $C_{th}$ denote the end-to-end throughput, then it has an upper bound as following,

$$C_{th} = \frac{W}{k} \quad (16)$$

where $W$ denotes the effective data rate achieved at each relay.

## IV. Simulation Evaluation of Tunable PCS

In this section, we present results from a series of simulations to demonstrate the effectiveness of physical carrier sensing with tunable sensing thresholds in improving network performance for various topologies. All the simulations were conducted in the OPNET simulation environment [12]. We have extended OPNET kernel modules to support tunable physical carrier sensing, a configurable propagation environment and multiple 802.11b data rates.

In all simulations, each node is always backlogged, each MAC data frame is 1024-byte long, and each node transmits at a fixed power of 0 dbm. By default, the OPNET simulator configures the physical carrier sensing threshold to be the same as the reception threshold. Furthermore, the ambient noise level is set at $-200$ dbm.

### A. Point-to-point baseline performance of 802.11b MAC

To quantitatively validate the effectiveness of physical carrier sensing, we need the following two baseline figures: the SNIR thresholds ($S_0$) required to sustain each available data rate in an 802.11b network, and the effective MAC throughput at each data rate. In the first simulation, we configured a network of two nodes – one sender and one

 0-7803-8533-0/04/$20.00 (c) 2004 IEEE

| Data Rate (Mbps) | 1 | 2 | 5.5 | 11 |
|---|---|---|---|---|
| $S_0$ (dB) | 11 | 14 | 18 | 21 |
| Throughput W (Mbps) | 0.89 | 1.5 | 3.5 | 5.0 |

TABLE I
SNIR REQUIREMENT VS. DATA RATE FOR 802.11B

receiver. The pathloss exponent was configured to be 2 to reflect a free-space environment. With RTS/CTS disabled, we varied the T-R separation distance and measured the effective throughput provided by the MAC layer at the receiver. The same simulation sequence was repeated for all four data rates defined in the 802.11b standard.

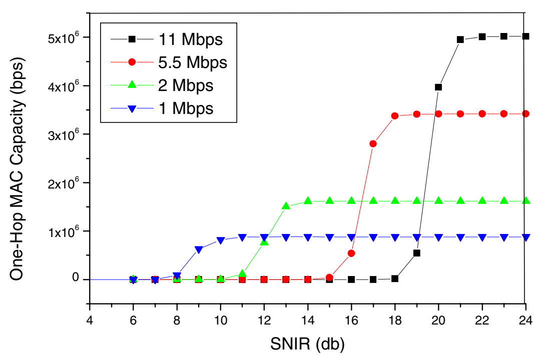


Fig. 2. Point-to-point throughput of an 802.11b link (RTS/CTS disabled).

The results are plotted in Fig.2. Instead of the T-R distance, we plotted the throughput against the SNIR at receiver. Hence the results depict the fundamental relationship between MAC throughput and receiver SNIR. This mapping is valid irrespective of pathloss exponent, transmission power and T-R distance. These results, recorded in Table I, will be used to design and analyze simulations in the rest of the section. The results demonstrate that MAC overhead is generally larger at higher data rates. Meanwhile, higher data rates require higher SNIR thresholds.

### *B. 4-node chain network*

Next we investigate a simple network where simultaneous communications may interfere with each other: a chain network with four nodes. In this experiment, the inter-node distance was a constant 12.5 meters and the receiving power threshold $P_R$ was configured to result in an effective transmission range of 13 meters. Hence a packet can only be correctly decoded by its immediate neighbor(s). In this topology, there are three representative patterns of immediate neighbor communication, as illustrated in Fig. 3, where the arrows indicate the direction of communication.

By default, the OPNET simulator sets the physical carrier sensing threshold ($P_C$) to be the same as the receiving threshold ($P_R$). Effectively the sensing range is equal to the receiving range, which reflects a common practice of current products on the market [13].

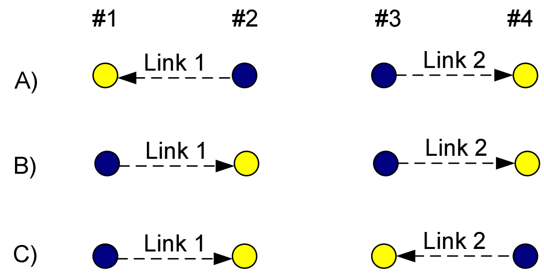


Fig. 3. Three representative scenarios in a four-node chain

To compare how different interference avoidance schemes affect the aggregate throughput in such a network, we simulated the following three combinations: (1) Virtual Carrier Sensing (VCS) with static Physical Carrier Sensing (PCS) – RTS/CTS enabled with $X = R$. (2) Tunable PCS only – RTS/CTS disabled. (3) VCS with tunable PCS – the PCS threshold was tested at $R$, $2R$ and $3R$. The data rate was set at 1 Mbps.

By looking at the directionality of the traffic in Fig. 3, it is intuitive to see that in order for one transmitter to sense the on-going transmission of the other, the sensing range (X) in the three scenarios should be R, 2R, and 3R, respectively. Hence we plot the aggregate throughput at the intuitively optimal sensing range for each scenario in Fig. 4.

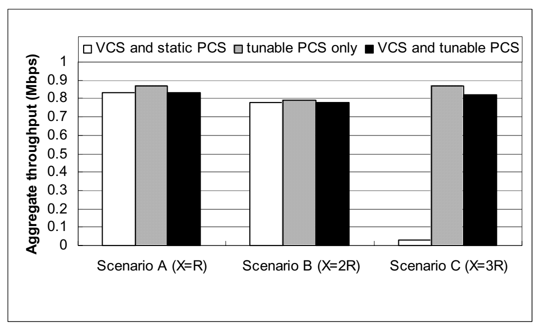


Fig. 4. Aggregate throughput in a four-node chain for scenarios in Fig.3

The most interesting result is in scenario C, where the optimally tuned physical sensing was able to achieve significantly better throughput (both with and without VCS) than virtual carrier sensing with the default static physical sensing threshold. This is because the transmitter in Link 2 (node 4) is outside of the transmission range of the RTS/CTS handshake of Link 1 (node 1 and 2). Hence it cannot decode either the RTS or CTS frame. Subsequently it would start transmission, and introduce interference. Node 1 would introduce interference to Link 2 for the same reason. Virtual carrier sensing with the default static physical sensing threshold was not able to avoid interference in that case. When the physical sensing threshold is tuned to be 3R, node 4 will be able to sense the transmission from node 1, and vice versa. Therefore interference was avoided and aggregate throughput was improved. Meanwhile, VCS does not allow such flexibility.

As the figure shows, in each of the three scenarios, tunable carrier sensing threshold (range) is a key factor for attaining the best aggregate throughput. Moreover, when the physical sensing threshold is tuned to the optimal value, enabling VCS did not further improve the throughput. On the contrary, VCS, in that case, introduced additional overhead that degraded the throughput. It is worth noting that the RTS/CTS mechanism has begun to be used for purposes beyond virtual carrier sensing, e.g. link layer channel measurement and training. However, from the standpoint of interference mitigation, our experiment results do not demonstrate a benefit of using VCS beyond that achieved from tuned PCS.

The best aggregate throughput in all three scenarios are between 0.8 Mbps and 0.9 Mbps. According to Table I, that value is very close to the optimal throughput at 1Mbps. Hence tunable physical sensing is beneficial regardless of traffic direction.

### *C. Large-scale chain network*

We expanded the previous network into a chain of 90 homogeneous nodes. Only end-to-end traffic going from node 1 to node 90 is generated. Each packet will be relayed by the 88 intermediate nodes before reaching its destination. Each node relies on physical carrier sensing only to avoid interference. We measured the end-to-end throughput while varying the sensing threshold and data rate shared by all nodes. A pathloss exponent of 2 was used to reflect a free-space propagation environment. The results are plotted in Fig. 5.

Notice in the figure that there exists an optimal sensing threshold value for each data rate. With everything else fixed, altering the data rate changes the SNIR requirement ($S_0$), hence the optimal sensing threshold changes as well. Also notice that the common practice of having the carrier sense threshold equal to the reception threshold is equivalent to having $P_{cs\_t} = 0db$, which corresponds to the right-most point on respective curves. Hence, the throughput improvement achieved by tunable physical carrier sensing threshold is significant for each data rate.

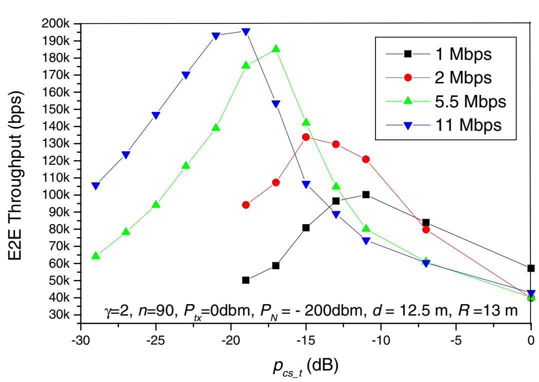


Fig. 5. End-to-end throughput in a 90-hop chain

Table II compares the optimal sensing thresholds $p_{cs\_t}$ obtained from the simulations against the two theoretical predictions: $\beta$ from (8) and $\beta'$ from (10). As the table shows, the three values are very close to each other. Hence the theoretical predictions are able to offer reasonable confidence in achieving the optimal end-to-end throughput in a chain network.

| Data Rate (Mbps) | 1 | 2 | 5.5 | 11 |
|---|---|---|---|---|
| Optimal $p_{cs\_t}$ (dB) | -11 | -15 | -17 | -19 |
| $\beta$ (dB) | -13 | -16 | -19 | -22 |
| $\beta'$ (dB) | -11 | -14 | -18 | -21 |

TABLE II

OPTIMAL SENSING THRESHOLDS IN A 90-NODE CHAIN

Next we compare the optimal throughput obtained from the simulations against the prediction from the spatial reuse study in (16). As shown in Table III, the optimal carrier sensing was able to achieve around 90% of the theoretical prediction. Therefore, given the assumptions of the simulations, any further enhancement to implement spatial reuse will not be able to provide more than 10% additional improvement to the network throughput.

| Data Rate (Mbps) | 1 | 2 | 5.5 | 11 |
|---|---|---|---|---|
| $W$ (Mbps) | 0.89 | 1.5 | 3.4 | 5.0 |
| $k$ (spatial reuse) | 7.1 | 10 | 15.9 | 22.4 |
| T: Theoretical ($W/k$) | 0.105 | 0.15 | 0.21 | 0.223 |
| S: Simulation | 0.1 | 0.134 | 0.185 | 0.196 |
| S/T | 95% | 89% | 88% | 88% |

TABLE III

OPTIMAL THROUGHPUT IN A 90-NODE CHAIN

### *D. 2-D grid network*

Finally, we investigated the effectiveness of tunable PCS in 2-D networks. We constructed a 20 by 20 grid. Each packet has its own destination that is chosen randomly from the immediate neighbors of the transmitter. The Manhattan distance between neighboring nodes 12.5 meters. Again, the reception power threshold ($P_R$) was configured such that the transmission range is 13 meters.

We conducted two sets of simulations using 1 Mbps and 11 Mbps data rate for each node, respectively. In each set of the simulations, we altered the pathloss exponent and PCS threshold. The aggregate throughput of the grid network are plotted in Fig. 6.

The figures clearly show that in each scenario, varying the PCS threshold has significant effect on the aggregate throughput of the grid network. Moreover, the optimal PCS threshold that leads to the best network throughput only depends on the data rate. The pathloss exponent doesn't alter the optimal threshold.

To further compare the effectiveness of PCS and VCS in leveraging spatial reuse, we enabled the VCS with $p_{cs\_t} = 0dB$, and run the simulation at 1 Mbps. We compare the

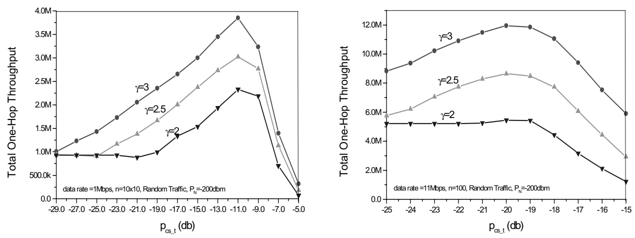


a) Data rate = 1Mbps b) Data rate = 11 Mbps

Fig. 6. Impact of PCS threshold on one-hop throughput in a grid

aggregate throughput to the optimal value obtained from tunable PCS. The results are plotted in Fig. 7. The figure shows that tunable PCS has a deciding advantage over VCS in mitigating interference. Furthermore, as the pathloss exponent increases, such advantage becomes more evident. Recall the spatial reuse results indicated in (15), a larger pathloss exponent will lead to a smaller $k$, i.e. better spatial reuse. PCS is able to leverage the increased potential in spatial reuse.

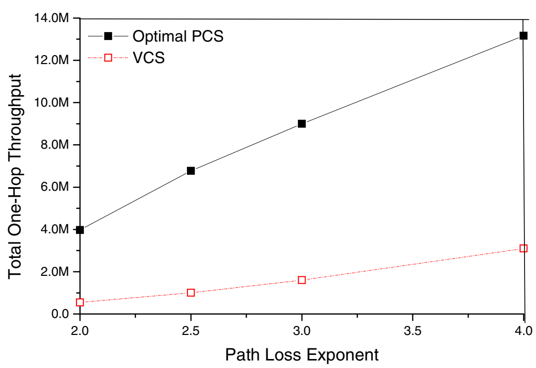


Fig. 7. Optimal PCS vs. VCS (data rate = 1Mbps)

## V. Related Work

Interference mitigation has been a well-known challenge for MAC protocols in wireless mesh networks. Much of the existing research in this space has been focusing on eliminating the *hidden terminal* [8] problem. A virtual carrier sensing mechanism, implemented through the RTS/CTS handshake, has been adopted by IEEE 802.11 in an attempt to eliminate the hidden terminal problem. However, this mechanism has an underlying assumption that all hidden terminals are within transmission range of receivers (allowing them to receive the CTS packet successfully). While such an assumption may be reasonable for single cell WLANs, it is generally not true for multi-cell WLANs and multi-hop mesh networks. Researchers [6] [9] [10] [11] have long recognized that RTS/CTS does not solve the hidden terminal problem effectively for such networks.

It was shown in both [9] and [11] that the interference range is a function of T-R separation distance. Depending on the T-R separation distance, the interference range can be smaller or larger than the transmission range. If the interference range is smaller than the transmission range, RTS/CTS can indeed prohibit all the hidden terminals from interfering with the existing transmission; but some of the nodes that are not capable of interfering are also prohibited from transmitting. Thus, in this configuration RTS/CTS becomes too aggressive, resulting in a significant exposed terminal problem that wastes potential throughput by requiring potential transmitters to unnecessarily back off. On the other hand, if the interference range is larger than the transmission range, RTS/CTS can fail to prevent hidden terminals from interfering with an existing transmission. So RTS/CTS becomes too conservative and ineffective in this case.

A technique was suggested in [9] to avoid the conservative RTS/CTS situation by allowing only the transmitter-receiver pairs with distance shorter than a threshold to perform transmission; the threshold is set such that the corresponding interference range will not be larger than the transmission range. The constraint on T-R separation distance is imposed by only allowing a node to reply to a RTS packet with a CTS packet when the receive power of the RTS packet is larger than a threshold, even if the RTS packet is received successfully and the node is idle. This added constraint ensures that RTS/CTS never becomes too conservative and so the hidden terminal problem is avoided. However, this approach does not address the exposed terminal problem introduced by the aggressive RTS/CTS. Another disadvantage of such an approach is that it reduces effective transmission range and thus lowers network connectivity.

Several other techniques attempt to reduce inefficiencies introduced by exposed terminals. The protocol described in [7] focuses on the exposed terminal problem directly by enabling nodes to identify themselves as exposed nodes and opportunistically scheduling concurrent transmissions whenever possible. While [11] recognizes that RTS/CTS can be either too conservative or too aggressive, it only directly addresses the problems associated with aggressive RTS/CTS. The authors propose a Distance-Aware Carrier Sensing (DACS) scheme which employs an extra handshake in addition to RTS/CTS to disseminate one-hop distance information to neighbors so that medium reservation can be more accurate and spatial reuse can be improved to reduce the negative impact of exposed terminals.

The unfairness introduced by EIFS based deferment when a hidden terminal senses RTS/CTS handshake in its sensing range but can not decode the packet and NAV correctly is explored in [6]. The authors proposed a method to convey the frame type information to hidden terminals even if the packet and NAV cannot be decoded correctly so that the hidden terminal can backoff more properly to improve the fairness.

Unlike prior techniques that attempt to avoid interference through handshake protocols, this paper approaches interference mitigation from the perspective of leveraging spatial reuse. We believe that the key to the optimal spatial reuse is to maintain the appropriate separation distance between simultaneous transmitters. Therefore we focus on enhancing the physical carrier sensing mechanism with tunable sensing threshold for the 802.11 MAC. What we proposed in this paper is a simple and effective technique that directly addresses the ineffectiveness of virtual carrier sensing with RTS/CTS.

## VI. Conclusion

In this paper, we proposed to enhance physical carrier sensing with tunable sensing threshold to improve spatial reuse in 802.11 mesh networks, aiming at increasing the aggregate network throughput. We derived two analytical estimations to the optimal sensing threshold – $\beta$ and $\beta'$. Simulations were performed for both chain and grid topologies to validate the estimations. Furthermore, tuning the carrier sensing does not require the modification to 802.11 MAC protocol. The main conclusions drawn from this paper are:

(1) Physical carrier sensing with the optimal sensing threshold is effective at leveraging spatial reuse in 802.11 multi-hop mesh networks, shown by increases in aggregate throughput. Such improvement does not require the use of virtual carrier sensing.

(2) Although the 802.11 MAC is a CSMA/CA based distributed and asynchronous scheme, it has the capability to make good use of the spatial-reuse property in a mesh (90% of the theoretical limit in a chain).

(3) $\beta' = 1/S_0$, the estimation to the optimal sensing threshold aiming at eliminating hidden terminals, is sufficient to achieve close-to-optimal performance in chain and grid topologies.

As the initial step to showcase the potential of enhanced physical carrier sensing, this paper focuses on symmetric network topologies consisting of homogeneous nodes. Future work may include extending the investigation to random topology, and with heterogeneous nodes (e.g. variable transmission power). Nonetheless, we have demonstrated in this paper that the sensing threshold should be independently tunable in 802.11 products, and the optimal threshold will lead to substantial improvement to 802.11 mesh networks.

## References


[1] IEEE Standard for Wireless LAN Medium Access Control (MAC) and Physical Layer (PHY) specifications, ISO/IEC 8802-11: 1999(E), Aug. 1999.

[2] B. P. Crow, J. G. Kim, IEEE 802.11 Wireless Local Area Networks, IEEE Comm. Mag., Sept. 1999.

[3] G. Bianchi, Performance Analysis of the IEEE 802.11 Distributed Coordination Function, IEEE JSAC, vol. 18, no. 3, March 2000.

[4] X. Guo, S. Roy, W. Steven Conner, Spatial Reuse in Wireless Ad-Hoc Networks, VTC2003.

[5] X. Guo, ”Personal research notes”, 2003.

[6] Z. Li, S. Nandi, and A. K. Gupta, Improving Fairness in IEEE 802.11 based MANETs using Enhanced Carrier Sensing, http://www.ntu.edu.sg/home5/pg03802331/papers/ecs.pdf.

[7] D. Shukla, L. Chandran-Wadia, S. Iyer, Mitigating the exposed node problem in IEEE 802.11 adhoc networks, IEEE ICCCN 2003, Dallas, Oct 2003.

[8] F. A. Tobagi, L. Kleinrock, Packet Switching in Radio Channels: PART II- The Hidden Terminal Problem in Carrier Sensing Multiple Access and Busy Tone Solution”, IEEE Trans. on Commun, Vol. COM-23, No. 12, pp. 1417-1433, 1975.

[9] K. Xu, M. Gerla, S. Bae, How effective is the IEEE 802.11 RTS/CTS handshake in ad hoc networks, GLOBECOM02, Nov 17-21, 2002.

[10] S. Xu, T. Saadawi, Does the IEEE 802.11 MAC Protocol Work Well in Multihop Wireless Ad Hoc Networks, IEEE Communications Magazine, P130-137, June 2001.

[11] F. Ye, B. Sikdar, Improving Spatial Reuse of IEEE 802.11 Based Ad Hoc Networks, To appear in the Proceedings of IEEE GLOBECOM, San Francisco, December 2003.

[12] http://www.opnet.com

[13] Intersil, Direct Sequence Spread Spectrum Baseband Processor, Doc# FN 4816.2, Feb. 2002, http://www.intersil.com/

[14] Theodore S. Rappaport, Wireless Communications, Principles and Practices, 2nd Ed. Prentice Hall, 2002. ISBN 0-13-042232-0